Density dependence of 2p-2h meson-exchange currents

J. E. Amaro,[1] M. B. Barbaro,[2,3] J. A. Caballero,[4] A. De Pace,[3] T. W. Donnelly,[5] G. D. Megias,[4] and I. Ruiz Simo[1]

[1]*Departamento de Física Atómica, Molecular y Nuclear, and Instituto de Física Teórica y Computacional Carlos I, Universidad de Granada, Granada 18071, Spain*

[2]*Dipartimento di Fisica, Università di Torino, Via P. Giuria 1, 10125 Torino, Italy*

[3]*INFN, Sezione di Torino, Via P. Giuria 1, 10125 Torino, Italy*

[4]*Departamento de Física Atómica, Molecular y Nuclear, Universidad de Sevilla, Apdo. 1065, 41080 Sevilla, Spain*

[5]*Center for Theoretical Physics, Laboratory for Nuclear Science and Department of Physics, Massachusetts Institute of Technology, Cambridge, Massachusetts 02139, USA*

(Received 28 April 2017; published 12 June 2017)

We analyze the density dependence of the contribution of meson-exchange currents to the lepton-nucleus inclusive cross section in the two-particle two-hole channel. The model is based on the relativistic Fermi gas, where each nucleus is characterized by its Fermi momentum k_F. We find that the 2p-2h nuclear response functions at their peaks scale as Ak_F^2 for Fermi momentum going from 200 to 300 MeV/c and momentum transfer q from $2k_F$ to 2 GeV/c. This behavior is different from what is found for the quasielastic response, which scales as A/k_F. Additionally, the deep scaling region is also discussed and there the usual scaling behavior is found to be preferable.

DOI: 10.1103/PhysRevC.95.065502

I. INTRODUCTION

Two-particle two-hole (2p-2h) excitations in electroweak nuclear reactions have been extensively explored in the past [1–19] in electron and neutrino scattering studies. These states, where two nucleons are promoted above the Fermi level leaving two holes inside the Fermi sea, are known to give a large contribution to the inclusive (e,e') cross section in the so-called "dip region", corresponding to excitation energies lying between the quasielastic (QE) and $\Delta(1232)$ excitation peaks.

This subject has received renewed attention in recent years, since 2p-2h excitations have been shown to play an important role in explaining neutrino-nucleus cross sections measured in neutrino oscillation experiments [20–25]. Whereas most of the existing calculations refer to a ^{12}C target [13,15,26–33], there is growing interest in the extension to heavier nuclei, such as ^{16}O, ^{40}Ar, ^{56}Fe, and ^{208}Pb, used in ongoing and future neutrino experiments. Since the calculation of the 2p-2h response is computationally demanding and time consuming, in this paper we provide an estimate of the density dependence of these contributions which can be used to extrapolate the results from one nucleus to another.

In [34,35] inclusive electron scattering data from various nuclei were analyzed in terms of "superscaling": it was shown that, for energy loss below the quasielastic peak, the scaling functions, represented versus an appropriate dimensionless scaling variable, are not only independent of the momentum transfer (scaling of first kind), but they also coincide for mass number $A \geqslant 4$ (scaling of second kind). More specifically, the reduced QE cross section was found to scale as A/k_F, k_F being the Fermi momentum. The Fermi momenta typical of most nuclei belong to the range 200–300 MeV/c [36]. It was also shown that for higher energy transfers superscaling is broken and that its violations reside in the transverse channel rather than in the longitudinal one. Such violations must be ascribed to reaction mechanisms different from one-nucleon knockout. Two-particle-two-hole excitations, which are mainly transverse and occur in the region between the quasielastic and Δ production peaks, are—at least in part—responsible for this violation.

In this paper we explore the k_F dependence of the 2p-2h nuclear response evaluated within the model of [10], based on the relativistic Fermi gas (RFG). The model has recently been extended to the weak sector [31] and applied to the study of neutrino-nucleus scattering. We refer the reader to the original papers for the details of the model. Here we just mention its main features: it is based on a fully relativistic Lagrangian including nucleons, pions, and Δ degrees of freedom; it involves the exact calculation of a huge number of diagrams, each of them involving a seven-dimensional integral; and it takes into account both direct and exchange Goldstone diagrams.

II. FORMALISM

The lepton-nucleus inclusive cross section can be described in terms of response functions, which embody the nuclear dynamics. There are two response functions in the case of electron scattering,

$$\frac{d^2\sigma}{d\Omega d\omega} = \sigma_{\rm Mott}[v_L R^L(q,\omega) + v_T R^T(q,\omega)], \tag{1}$$

and five in the case of charged-current (anti)neutrino scattering,

$$\frac{d\sigma}{dk' d\Omega} = \sigma_0[\hat{V}_{CC} R^{CC}(q,\omega) + 2\,\hat{V}_{CL} R^{CL}(q,\omega) + \hat{V}_{LL} R^{LL}(q,\omega) + \hat{V}_T R^T(q,\omega) \pm 2\hat{V}_{T'} R^{T'}(q,\omega)]. \tag{2}$$

In the above $\sigma_{\rm Mott}$ is the Mott cross section, σ_0 the analogous quantity for neutrino scattering, q and ω the momentum and energy transferred to the nucleus, Ω and k' the outgoing lepton solid angle and momentum, and v_K, $\hat{V}_K$ kinematical factors that only depend on the leptonic variables (see [37] for their explicit expressions). The $\pm$ sign in Eq. (2) refers to neutrino and antineutrino scattering, respectively. We shall denote by $R^K_{\rm MEC}$ the contribution to the response R^K arising from the excitation of 2p-2h states induced by meson-exchange currents (MEC).

In order to remove the single-nucleon physics from the problem (which also causes the fast growth of the response as ω approaches the light-cone), it is useful to define the following reduced response (per nucleon):

$$F^T_{\rm MEC}(q,\omega) \equiv \frac{R^T_{\rm MEC}(q,\omega)}{\widetilde{G}^2_M(\tau)}\,, \tag{3}$$

where $\tau \equiv (q^2-\omega^2)/(4m_N^2)$ and

$$\widetilde{G}^2_M(\tau) \equiv Z G^2_{Mp}(\tau) + N G^2_{Mn}(\tau)\,, \tag{4}$$

G_{Mp} and G_{Mn} being the proton and neutron magnetic form factors. For simplicity here we neglect in the single-nucleon dividing factor small contributions coming from the motion of the nucleons, where the electric form factor contributes, which depend on the Fermi momentum [38].

Since the behavior with density of the nuclear response is not expected to depend very much on the specific channel or on the nature of the probe, for sake of illustration we focus on the electromagnetic 2p-2h transverse response, which largely dominates over the longitudinal one. Our starting point is therefore the electromagnetic transverse response, $R^T_{\rm MEC}$, associated with meson-exchange currents (MEC) carried by the pion and by the Δ resonance, evaluated within the model of [10].

III. RESULTS

In the results shown here we take $Z = N$ and we use the Hoeler parametrization for the proton and neutron magnetic form factors. The case of asymmetric nuclei, $Z \neq N$, requires more involved formalism and will be addressed in future work, although preliminary studies indicate that the qualitative behavior with k_F does not change dramatically unless $N - Z$ is very large. In particular, the present study can yield valuable information on how to extrapolate the results obtained for scattering on ^{12}C not only to ^{16}O but also to ^{40}Ar, a nucleus widely used in ongoing and future neutrino experiments.

In Fig. 1 we display $R^T_{\rm MEC}$ as a function of the energy transfer ω for momentum transfers q ranging from 50 to 2000 MeV/c and three values of the Fermi momentum k_F from 200 to 300 MeV/c.

To illustrate the k_F behavior of the response, we now fix the momentum transfer to a specific value. In the upper panels of Fig. 2 we show the response $R^T_{\rm MEC}$ and the reduced response $F^T_{\rm MEC}$ for $q = 800$ MeV/c and the same three values of k_F used above. It clearly appears that the 2p-2h response, unlike the one-body quasielastic one, increases as the Fermi momentum increases. In the lower panels of Fig. 2 we display the scaled 2p-2h MEC response, defined as

$$\widetilde{F}^T_{\rm MEC}(\psi'_{\rm MEC}) \equiv \frac{F^T_{\rm MEC}}{\eta_F^2}\,, \tag{5}$$

namely, the reduced response divided by $\eta_F^2 \equiv (k_F/m_N)^2$, as a function of the MEC scaling variable $\psi'_{\rm MEC}(q,\omega,k_F)$ (left panel) and of the quasielastic one $\psi'_{\rm QE}(q,\omega,k_F)$ (right panel). The MEC scaling variable is defined in the Appendix, in analogy with the usual QE scaling variable [38]. The results show that the reduced 2p-2h response roughly scales as k_F^2 when represented as a function of $\psi'_{\rm MEC}$ [Fig. 2(c)], i.e., the scaled 2p-2h MEC response shown there coalesces at the peak into a universal result. This scaling law is very accurate at the peak of the 2p-2h response, while it is violated to some extent at large negative values of the scaling variable. Figure 2(d) shows that in this "deep scaling" region it is more appropriate to use the usual scaling variable $\psi'_{\rm QE}$ devised for quasielastic scattering. This latter region was previously investigated in [11]: in that study the specific cases of ^{12}C ($k_F = 228$ MeV/c) and ^{197}Au($k_F = 245$ MeV/c) were considered and the superscaling functions f were plotted versus ψ' ($f^T_{\rm MEC}$ and $\psi'_{\rm QE}$ in the present work) together with JLab data at electron energy $\epsilon = 4.045$ GeV and scattering angle $\theta = 23^\circ$ and 30°— see Fig. 7 in [11]. Following [11]

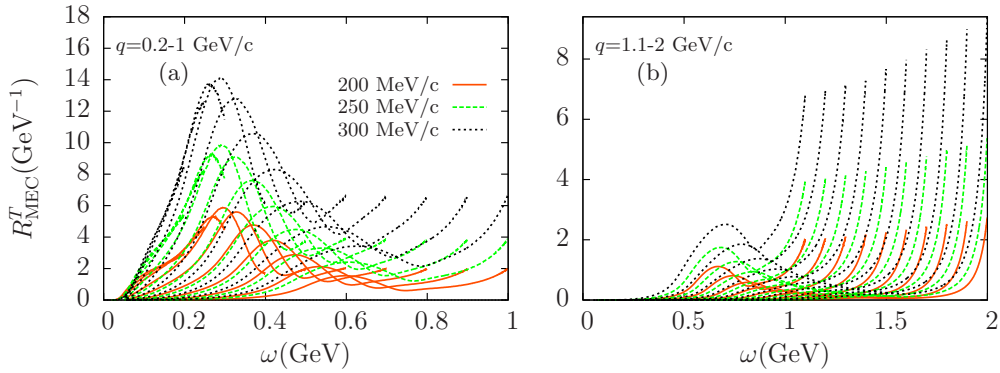

FIG. 1. The 2p-2h MEC response of [10] plotted versus ω for three values of the Fermi momentum k_F and for different values of the momentum transfer $q = 200, ..., 1000$ MeV/c (left panel) and 1100, ..., 2000 MeV/c (right panel), increasing from left to right.

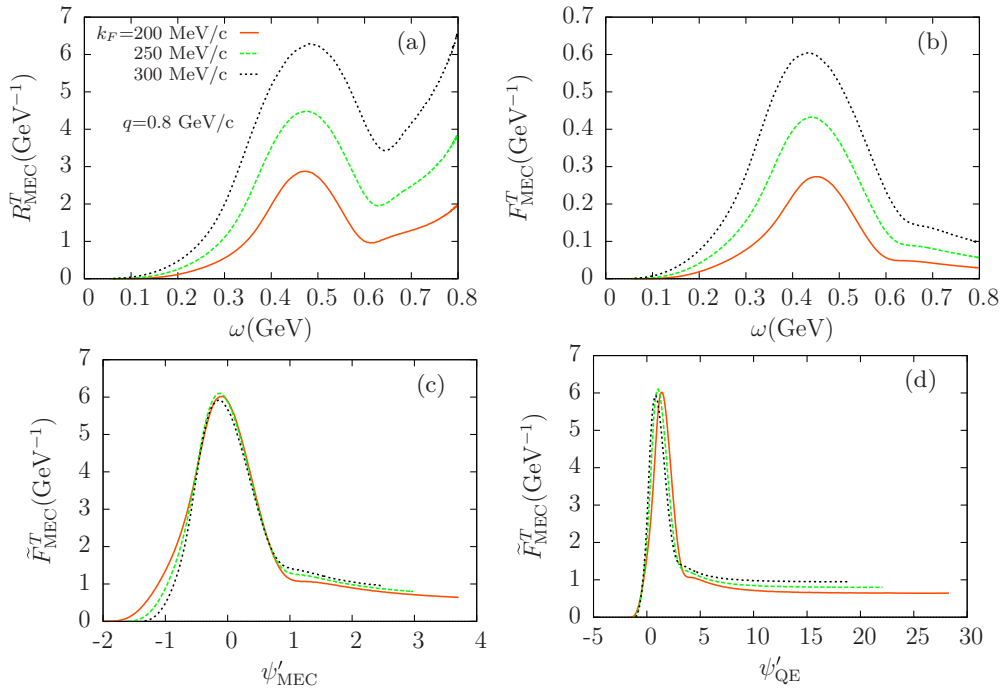

FIG. 2. Upper panels: The 2p-2h MEC response (a) and the reduced response defined by Eq. (3) (b) plotted versus ω for $q = 800\,\mathrm{MeV}/c$ and Fermi momentum k_F varying between 200 (lower curve) and 300 (upper curve) MeV/c. Lower panels: The corresponding scaled 2p-2h MEC response defined by Eq. (5) plotted versus the scaling variables $\psi'_{\rm MEC}$ (c) and $\psi'_{\rm QE}$ (d).

$f^T_{\rm MEC}$ is defined by

$$f^T_{\rm MEC} \equiv F^T_{\rm MEC} \times k_F\,. \tag{6}$$

There one observes two things: (1) the usual scaling, i.e., *not* the scaling behavior found in the present study at the peak of the MEC response, is reasonably compatible with the spread found in the data, and (2) at very high momentum transfers the 2p-2h MEC contributions are very significant in this deep scaling region, to the extent that they may even provide the dominant effect.

For completeness, in Fig. 3 we show results at $q = 2\,\mathrm{GeV}/c$ using the two types of k_F-scaling behavior. In particular, in the right-hand panel where the usual superscaling results are presented it should be emphasized that, for the most negative values of $\psi'_{\rm QE}$ (the deep scaling region), the data analyzed in [11] fall well inside the range spanned by the upper curve ($k_F = 200\,\mathrm{MeV}/c$) and the middle curve ($k_F = 250\,\mathrm{MeV}/c$).

In Fig. 4 the scaled 2p-2h MEC response is now plotted versus $\psi'_{\rm MEC}$ for four values of q. Here we see that the same k_F dependence is valid for different values of q as long as Pauli blocking is not active, namely $q > 2k_F$. At lower q and in the deep scaling region this type of scaling is seen to be broken (see also above).

A closer inspection of the scaling properties of the 2p-2h response is presented in Figs. 5–7. In Fig. 5 the separate contributions of $\Delta\Delta$-, $\pi\pi$-, and $\pi\Delta$-interference terms are displayed for two values of q and two values of k_F. In Fig. 6 the corresponding scaled responses are displayed as functions of the variable $\psi'_{\rm MEC}$: it appears that all contributions roughly

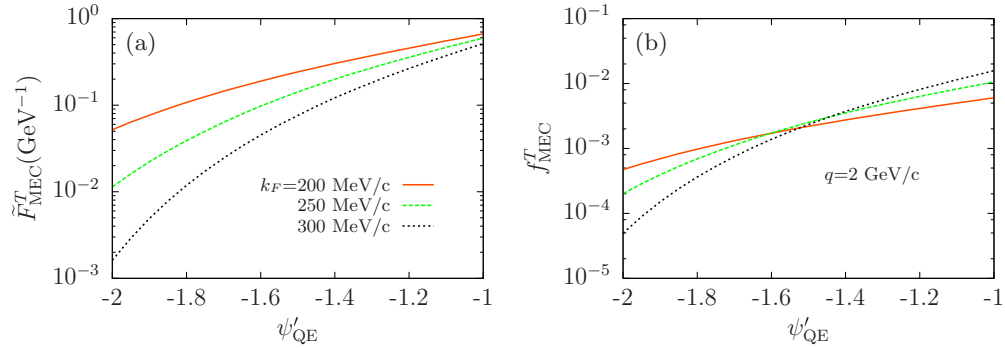

FIG. 3. The scaled 2p-2h MEC response defined by Eq. (5) (left panel) and the corresponding superscaling function defined by Eq. (6) (right panel) plotted versus the scaling variable $\psi'_{\rm QE}$ for $q = 2\,\mathrm{GeV}/c$.

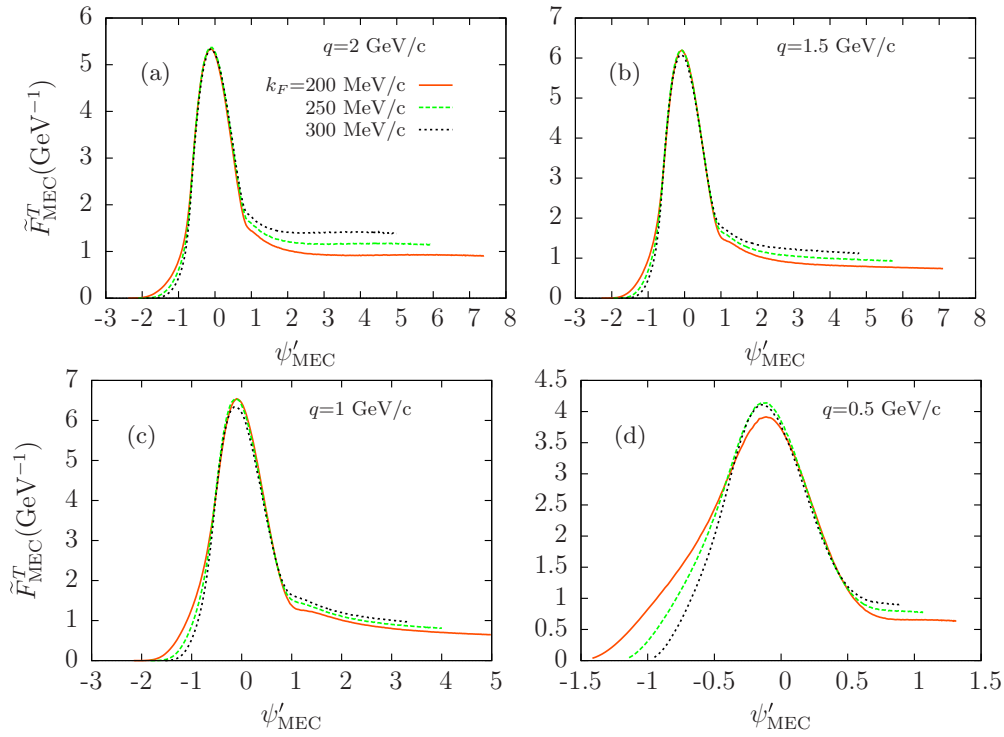

FIG. 4. As for Fig. 2(c), but now for different values of q.

grow as k_F^2, the quality of scaling being better for the $\Delta\Delta$ piece than for the other two contributions. It is interesting to observe that at high momentum transfer the total MEC response scales better than the pure Δ piece around the peak, indicating a compensation of scaling violations between the three terms. We notice that scaling violations are more sizable away from the peak: in Fig. 7 it is shown that in this region the quasielastic scaling variable, which appears to be more suitable to describe

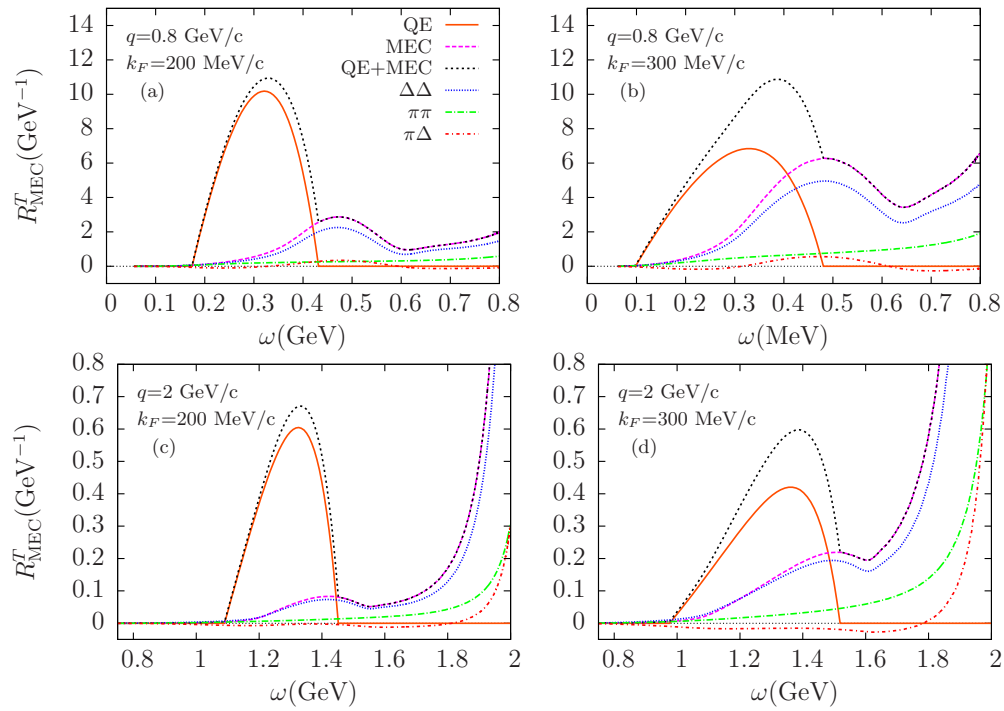

FIG. 5. The 2p-2h MEC transverse response $R^T_{\rm MEC}$ and the separate $\Delta\Delta$-, $\pi\pi$-, and $\pi\Delta$-interference components plotted versus ω. The free RFG transverse response (red curves) is also shown for reference.

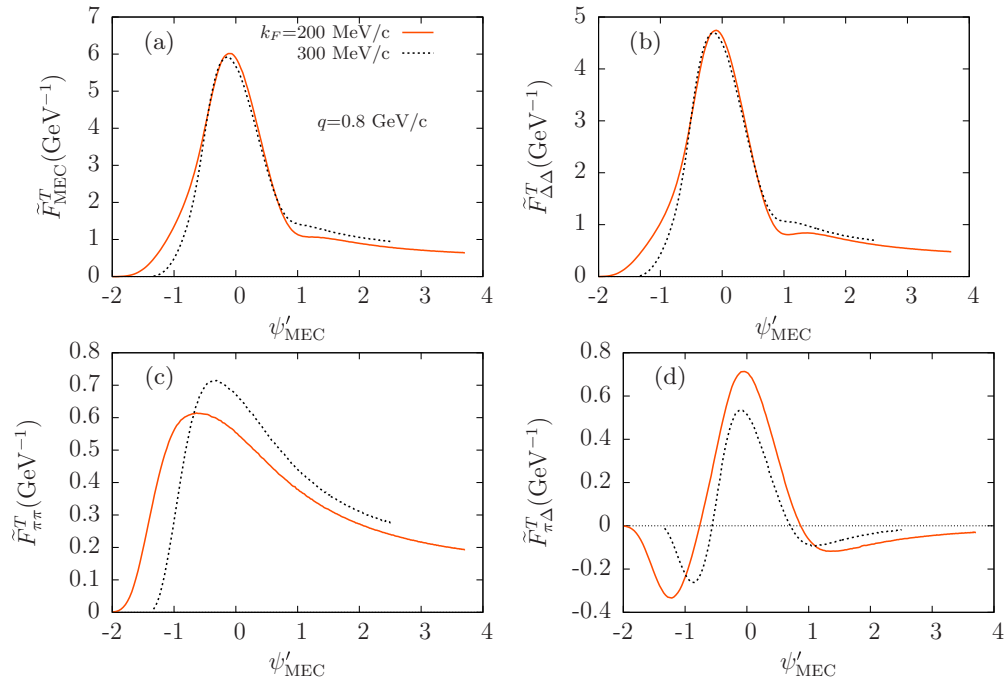

FIG. 6. The scaled 2p-2h MEC response $\widetilde{F}^T_{\rm MEC}$ defined in Eq. (5) and the separate $\Delta\Delta$-, $\pi\pi$-, and $\pi\Delta$-interference components plotted versus $\psi'_{\rm MEC}$ for $q = 800\,{\rm MeV}/c$ and $k_F = 200$ and $300\,{\rm MeV}/c$.

the pure pionic ($\pi\pi$) and interference ($\pi\Delta$) terms, gives a better scaling of second kind.

Finally, focusing on practical cases, in Fig. 8 we show $R^T_{\rm MEC}$ versus ω, together with $\widetilde{F}^T_{\rm MEC}$ and $f^T_{\rm MEC}$ versus $\psi'_{\rm qe}$ for three values of q and for the symmetric nuclei ^{4}He, ^{12}C, ^{16}O, and ^{40}Ca. The cases of ^{12}C and ^{16}O are clearly relevant for ongoing neutrino oscillation studies, whereas the case of ^{40}Ca is a symmetric nucleus lying close to the important case of ^{40}Ar. For comparison, ^{4}He is also displayed and, despite its small mass, is seen to be "typical". In contrast, the case of ^{2}H, whose Fermi momentum is unusually small ($k_F = 55\,{\rm MeV}/c$), was also explored and found to be completely anomalous: the

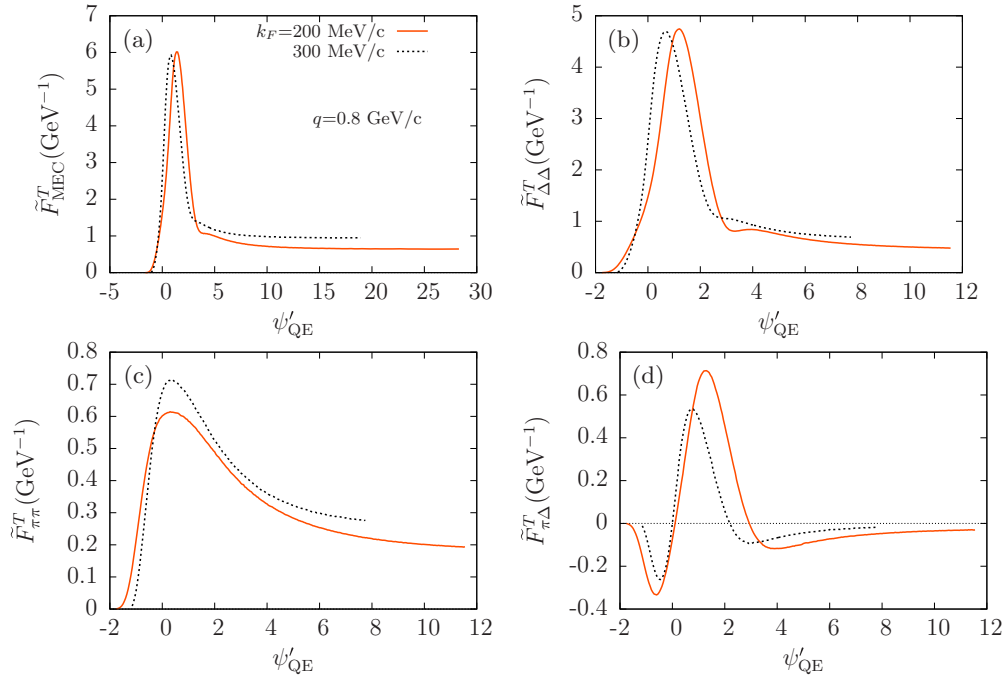

FIG. 7. The scaled 2p-2h MEC response $\widetilde{F}^T_{\rm MEC}$ defined in Eq. (5) and the separate $\Delta\Delta$-, $\pi\pi$-, and $\pi\Delta$-interference components plotted versus $\psi'_{\rm QE}$ for $q = 800\,{\rm MeV}/c$ and $k_F = 200$ and $300\,{\rm MeV}/c$.

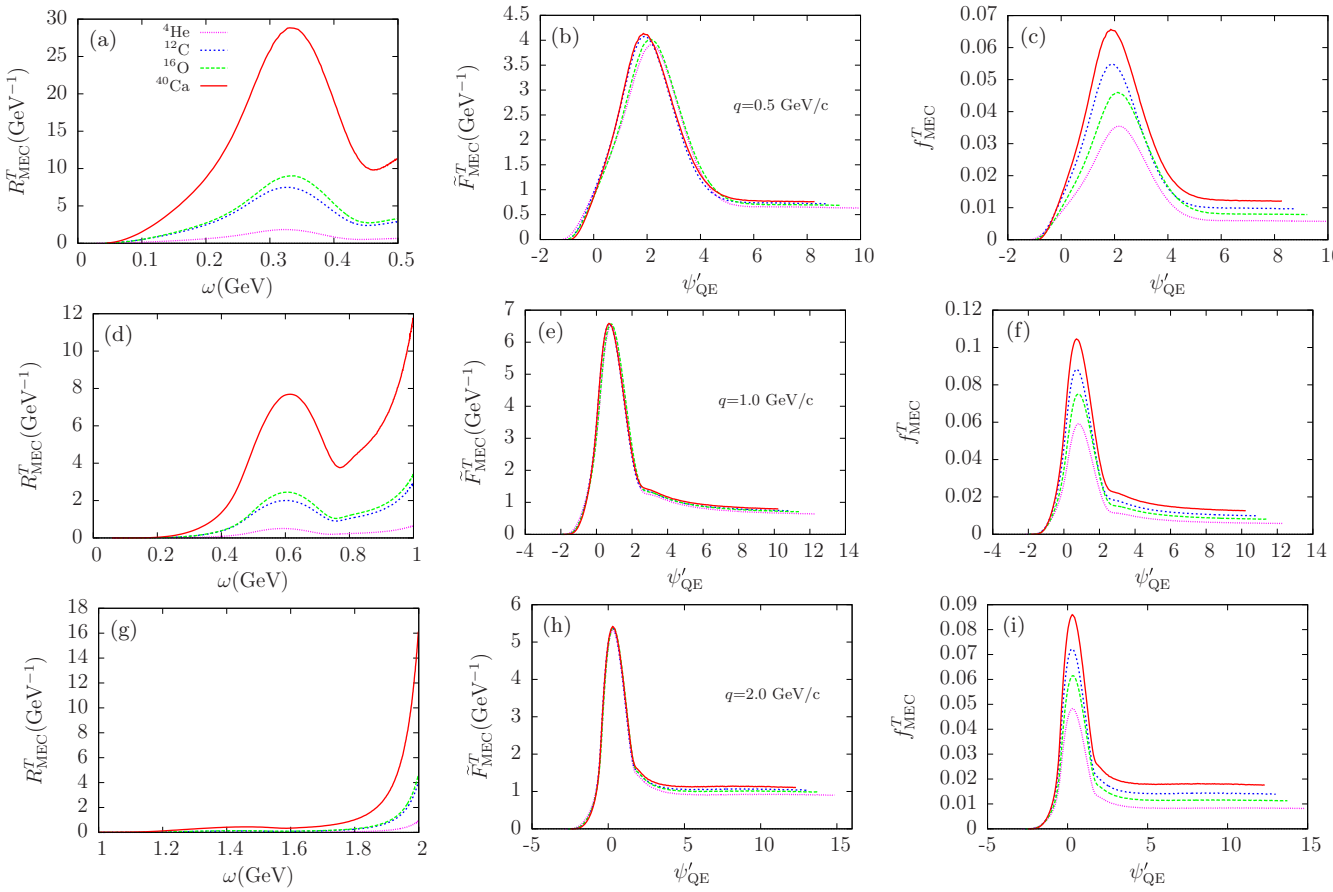

FIG. 8. The 2p-2h MEC response (first column), the corresponding scaled response $\widetilde{F}^T_{\rm MEC}$ defined by Eq. (5) (second column), and the superscaling function defined by Eq. (6) (third column) for four nuclei and three values of momentum transfer q.

MEC responses ($R^T_{\rm MEC}$) and superscaling results ($f^T_{\rm MEC}$) were both too small to show in the figure.

IV. CONCLUSIONS

Summarizing, we have shown that the 2p-2h MEC response function per nucleon roughly grows as k_F^2 for Fermi momenta varying from 200 to 300 MeV/c. This scaling law is excellent around the MEC peak for high values of q, it starts to break down around $q = 2k_F$, and gets worse and worse as q decreases. This behavior must be compared with that of the one-body response, which scales as $1/k_F$: hence the relative importance of the 2p-2h contribution grows as k_F^3. This result allows one to get an estimate of the relevance of these contributions for a variety of nuclei, of interest in ongoing and future neutrino scattering experiments, and should facilitate the implementation of 2p-2h effects in Monte Carlo generators. Finally, in the deep scaling region the MEC response is found to be significant and to scale not as k_F^2, but rather more as $1/k_F$.

ACKNOWLEDGMENTS

This work has been partially supported by the Instituto Nazionale di Fisica Nucleare (INFN) under project MANYBODY, by the Spanish Ministerio de Economia y Competitividad and ERDF (European Regional Development Fund) under Contracts No. FIS2014-59386-P, FIS2014-53448-C2-1, by the Junta de Andalucia (Grants No. FQM-225 and No. FQM160), and part (T.W.D.) by the U.S. Department of Energy under cooperative Agreement No. DE-FC02-94ER40818. I.R.S. acknowledges support from a Juan de la Cierva-incorporacion program from Spanish MINECO. G.D.M. acknowledges support from a Junta de Andalucia program (FQM7632, Proyectos de Excelencia 2011).

APPENDIX

The MEC scaling variable is defined as

$$\psi'_{\rm MEC}(q,\omega,k_F) \equiv \frac{1}{\sqrt{\xi_F^{\rm eff}(q)}} \times \frac{\lambda'_{\rm MEC} - \tau'_{\rm MEC}\rho'_{\rm MEC}}{\sqrt{(1+\lambda'_{\rm MEC}\rho'_{\rm MEC})\tau'_{\rm MEC} + \kappa\sqrt{\tau'_{\rm MEC}\left(1+\tau'_{\rm MEC}\rho'^2_{\rm MEC}\right)}}}, \quad \text{(A1)}$$

where

$$\lambda'_{\rm MEC} \equiv \frac{\omega'_{\rm MEC}}{2m_N}, \quad \kappa \equiv \frac{q}{2m_N}, \quad \tau'_{\rm MEC} \equiv \kappa^2 - (\lambda'_{\rm MEC})^2,$$
$$\omega'_{\rm MEC} \equiv \omega - E^{\rm shift}_{\rm MEC}(q), \quad \rho'_{\rm MEC} \equiv 1 + \frac{1}{4\tau'_{\rm MEC}}\left(\frac{m_*^2}{m_N^2} - 1\right). \tag{A2}$$

The functions

$$\xi_F^{\rm eff}(q) = \sqrt{1 + [\alpha(1 + \beta e^{-w\gamma})\eta_F]^2} - 1 \tag{A3}$$

and

$$E^{\rm shift}_{\rm MEC}(q) = E_0 + E_1 t + E_2 t^2 \tag{A4}$$

TABLE I. The parameters entering the definition of $\psi'_{\rm MEC}$ for ^{12}C.

m_*(MeV/c^2)	α	β	γ	E_0(MeV)	E_1(MeV)	E_2(MeV)
1170	1.3345	30.73	0.85	42.718	−70.0	37.0

with $w = q/1000$ and $t = (q - 500)/1000$ with q in MeV/c are chosen in such a way that the maxima of the 2p-2h response at different values of q align at $\psi'_{\rm MEC} = 0$. The values of the parameters for the case of ^{12}C are given in Table I; the same values are used for all the choices of k_F and the results shown in Fig. 4 indicate that this procedure is successful.

The usual definition of $\psi'_{\rm QE}$ can be recovered from the above equations by setting $m_* = m_N$ (hence $\rho' = 1$).

[1] J. W. Van Orden and T. W. Donnelly, Ann. Phys. (NY) **131**, 451 (1981).
[2] W. M. Alberico, M. Ericson, and A. Molinari, Ann. Phys. (NY) **154**, 356 (1984).
[3] J. E. Amaro, G. Co', and A. M. Lallena, Ann. Phys. (NY) **221**, 306 (1993).
[4] J. E. Amaro, A. M. Lallena, and G. Co, Nucl. Phys. A **578**, 365 (1994).
[5] W. M. Alberico, A. De Pace, A. Drago, and A. Molinari, Riv. Nuovo Cimento **14**, 1 (1991).
[6] A. Gil, J. Nieves, and E. Oset, Nucl. Phys. A **627**, 543 (1997).
[7] M. J. Dekker, P. J. Brussaard, and J. A. Tjon, Phys. Lett. B **266**, 249 (1991).
[8] M. J. Dekker, P. J. Brussaard, and J. A. Tjon, Phys. Lett. B **289**, 255 (1992).
[9] M. J. Dekker, P. J. Brussaard, and J. A. Tjon, Phys. Rev. C **49**, 2650 (1994).
[10] A. De Pace, M. Nardi, W. M. Alberico, T. W. Donnelly, and A. Molinari, Nucl. Phys. A **726**, 303 (2003).
[11] A. De Pace, M. Nardi, W. M. Alberico, T. W. Donnelly, and A. Molinari, Nucl. Phys. A **741**, 249 (2004).
[12] M. Martini, M. Ericson, G. Chanfray, and J. Marteau, Phys. Rev. C **81**, 045502 (2010).
[13] J. Nieves, I. R. Simo, and M. J. Vicente Vacas, Phys. Rev. C **83**, 045501 (2011).
[14] J. Nieves, I. Ruiz Simo, and M. J. Vicente Vacas, Phys. Lett. B **707**, 72 (2012).
[15] J. E. Amaro, M. B. Barbaro, J. A. Caballero, T. W. Donnelly, and C. F. Williamson, Phys. Lett. B **696**, 151 (2011).
[16] J. E. Amaro, M. B. Barbaro, J. A. Caballero, and T. W. Donnelly, Phys. Rev. Lett. **108**, 152501 (2012).
[17] T. Van Cuyck, N. Jachowicz, R. Gonzalez-Jimenez, M. Martini, V. Pandey, J. Ryckebusch, and N. Van Dessel, Phys. Rev. C **94**, 024611 (2016).
[18] T. Van Cuyck, N. Jachowicz, R. González-Jiménez, J. Ryckebusch, and N. Van Dessel, Phys. Rev. C **95**, 054611 (2017).
[19] J. E. Amaro, C. Maieron, M. B. Barbaro, J. A. Caballero, and T. W. Donnelly, Phys. Rev. C **82**, 044601 (2010).
[20] A. A. Aguilar-Arevalo *et al.* (MiniBooNE Collaboration), Phys. Rev. D **81**, 092005 (2010).
[21] A. A. Aguilar-Arevalo *et al.* (MiniBooNE Collaboration), Phys. Rev. D **88**, 032001 (2013).
[22] P. A. Rodrigues *et al.* (MINERvA Collaboration), Phys. Rev. Lett. **116**, 071802 (2016).
[23] G. A. Fiorentini *et al.* (MINERvA Collaboration), Phys. Rev. Lett. **111**, 022502 (2013).
[24] K. Abe *et al.* (T2K Collaboration), Phys. Rev. D **87**, 092003 (2013).
[25] K. Abe *et al.* (T2K Collaboration), Phys. Rev. D **90**, 052010 (2014).
[26] M. Martini, M. Ericson, G. Chanfray, and J. Marteau, Phys. Rev. C **80**, 065501 (2009).
[27] O. Benhar, A. Lovato, and N. Rocco, Phys. Rev. C **92**, 024602 (2015).
[28] N. Rocco, A. Lovato, and O. Benhar, Phys. Rev. C **94**, 065501 (2016).
[29] G. D. Megias, J. E. Amaro, M. B. Barbaro, J. A. Caballero, and T. W. Donnelly, Phys. Rev. D **94**, 013012 (2016).
[30] G. D. Megias, J. E. Amaro, M. B. Barbaro, J. A. Caballero, T. W. Donnelly and I. R. Simo, Phys. Rev. D **94**, 093004 (2016).
[31] I. Ruiz Simo, J. E. Amaro, M. B. Barbaro, A. De Pace, J. A. Caballero, and T. W. Donnelly, J. Phys. G **44**, 065105 (2017).
[32] I. Ruiz Simo, J. E. Amaro, M. B. Barbaro, J. A. Caballero, G. D. Megias, and T. W. Donnelly, Phys. Lett. B **770**, 193 (2017).
[33] T. Katori and M. Martini, arXiv:1611.07770 [hep-ph].
[34] T. W. Donnelly and I. Sick, Phys. Rev. Lett. **82**, 3212 (1999).
[35] T. W. Donnelly and I. Sick, Phys. Rev. C **60**, 065502 (1999).
[36] C. Maieron, T. W. Donnelly, and I. Sick, Phys. Rev. C **65**, 025502 (2002).
[37] J. E. Amaro, M. B. Barbaro, J. A. Caballero, T. W. Donnelly, A. Molinari, and I. Sick, Phys. Rev. C **71**, 015501 (2005).
[38] W. M. Alberico, A. Molinari, T. W. Donnelly, E. L. Kronenberg, and J. W. Van Orden, Phys. Rev. C **38**, 1801 (1988).